Regulatory Role of Phospholamban in the Efficiency of Cardiac Sarcoplasmic Reticulum Ca^{2+} Transport†

Konrad Frank,‡ Carola Tilgmann,‡ Thomas R. Shannon,§ Donald M. Bers,§ and Evangelia G. Kranias*,‡

Department of Pharmacology and Cell Biophysics, University of Cincinnati College of Medicine, Cincinnati, Ohio 45267, and Department of Physiology, Loyola University Chicago, Maywood, Illinois 60153

Received May 8, 2000; Revised Manuscript Received September 21, 2000

ABSTRACT: Phospholamban is an inhibitor of the sarcoplasmic reticulum Ca^{2+} transport apparent affinity for Ca^{2+} in cardiac muscle. This inhibitory effect of phospholamban can be relieved through its phosphorylation or ablation. To better characterize the regulatory mechanism of phospholamban, we examined the initial rates of Ca^{2+}-uptake and Ca^{2+}-ATPase activity under identical conditions, using sarcoplasmic reticulum-enriched preparations from phospholamban-deficient and wild-type hearts. The apparent coupling ratio, calculated by dividing the initial rates of Ca^{2+} transport by ATP hydrolysis, appeared to increase with increasing [Ca^{2+}] in wild-type hearts. However, in the phospholamban-deficient hearts, this ratio was constant, and it was similar to the value obtained at high [Ca^{2+}] in wild-type hearts. Phosphorylation of phospholamban by the catalytic subunit of protein kinase A in wild-type sarcoplasmic reticulum also resulted in a constant value of the apparent ratio of Ca^{2+} transported per ATP hydrolyzed, which was similar to that present in phospholamban-deficient hearts. Thus, the inhibitory effects of dephosphorylated phospholamban involve decreases in the apparent affinity of sarcoplasmic reticulum Ca^{2+} transport for Ca^{2+} and the efficiency of this transport system at low [Ca^{2+}], both leading to prolonged relaxation in myocytes.

Phospholamban, a 52-amino acid phosphoprotein, is a prominent regulator of sarcoplasmic reticulum (SR)[1] Ca^{2+}-ATPase (SERCA2) activity and contractility (*1*−*3*). The functional role of phospholamban has been recently elucidated through the generation and characterization of a phospholamban-deficient mouse (*4*). This model exhibited significant decreases in the apparent EC_{50} values for Ca^{2+} of the SR Ca^{2+}-uptake and increases in cardiac contractile parameters (*4*). The hyperdynamic cardiac function was not associated with any compensatory alterations in Ca^{2+} handling proteins, with the exemption of the ryanodine receptor, which was downregulated (25%) (*5*). Oxygen consumption and the active form of the mitochondrial pyruvate dehydrogenase were also increased, without any changes in intracellular ATP levels, indicating an increased ATP turnover rate in the hyperdynamic phospholamban-deficient hearts (*5*). However, there was no compromise in exercise capacity (*6*) or life span of the phospholamban-deficient mice (*7*). On the basis of these findings, it was suggested that inhibition of phospholamban activity in vivo may represent an attractive method to increase cardiac contractility in heart disease (*1*−*3*).

The functional unit of phospholamban and the mechanism by which it mediates its regulatory effects in vivo are presently unknown. Dephosphorylated phospholamban has been proposed to interact with and reduce the apparent affinity of SERCA2 for Ca^{2+} (*8*, *9*). Phosphorylation of phospholamban during β-agonist stimulation of the heart removes its inhibition and facilitates Ca^{2+} transport into the SR lumen, enhancing cardiac relaxation (*10*, *11*). Using monoclonal antibodies to disrupt the interaction of phospholamban with SERCA2, it was demonstrated that phospholamban modulates the slow isometric transition produced by Ca^{2+} binding to the SR Ca^{2+}-ATPase (*12*). Furthermore, time-resolved phosphorescence anisotropy studies indicated that dephosphorylated phospholamban mediates aggregation of the SERCA2 molecules, resulting in a slow-down of the rate-limiting step of the enzymatic cycle (*13*).

The regulatory effects of phospholamban involve the cytoplasmic domain of the protein, and site-directed mutagenesis studies showed that specific hydrophilic residues among amino acids 2−18 in phospholamban interact with amino acids 336−412 in SERCA2 for functional modification (*14*). The hydrophobic domain is also important in mediating the regulatory effects of phospholamban (*15*), and it is responsible for pentameric assembly of the protein (*16*, *17*). Furthermore, previous studies have indicated that pentameric phospholamban may also form Ca^{2+} selective

† This study was supported by the National Institutes of Health Grants HL-26057, P40RR12358, HL-52318 (to E.G.K.), and HL-30077 (to D.M.B.) and a research fellowship grant of the Deutsche Forschungsgemeinschaft (FR-1466, K.F.).

* To whom correspondence should be addressed. Evangelia G. Kranias, Ph.D., Department of Pharmacology & Cell Biophysics, College of Medicine, University of Cincinnati, 231 Bethesda Avenue, P.O. Box 670575, Cincinnati, OH 45267-0575. Telephone: 513-558-2327. Fax: 513-558-2269. E-mail: kraniaeg@email.uc.edu.

‡ University of Cincinnati College of Medicine.

§ Loyola University Chicago.

[1] Abbreviations: EC_{50}: concentration for half-maximal activation; PKA: cAMP-dependent protein kinase A; PLB-KO: phospholamban-deficient; SERCA2: sarcoplasmic reticulum Ca^{2+}-ATPase, isoform 2; SR: sarcoplasmic reticulum; V_{max}: maximal Ca^{2+}-ATPase activity and Ca^{2+}-uptake; WT: wild-type.

10.1021/bi001049k CCC: $19.00
Published on Web 10/21/2000

channels in lipid bilayers (*18*). The putative transmembrane domain responsible for pentamerization and channel properties of phospholamban is composed of bulky hydrophobic amino acids and three cysteine residues (Cys^{36}, Cys^{41}, and Cys^{46}). Extensive mutagenesis studies (*17*) and consequent modeling (*19*) revealed that phospholamban pentameric formation is a left-handed coiled-coil configuration, with a cylindrical ion pore. However, the functional relevance of this ion channel and its implications in intracellular Ca^{2+} homeostasis remain poorly understood.

The present study was undertaken to provide additional insights into the regulatory mechanisms of phospholamban in cardiac SR function. Our findings demonstrate that ablation or cAMP-dependent phosphorylation of phospholamban in murine SR preparations results in increased efficiency of the Ca^{2+} transport system at low Ca^{2+} concentrations, suggesting an additional regulatory role of phospholamban at diastolic calcium concentrations in cardiac muscle.

EXPERIMENTAL PROCEDURES

Sarcoplasmic Reticulum-Enriched Membrane Preparations. Phospholamban-deficient and wild-type mice were sacrificed by cervical dislocation, the hearts were quickly excised and placed in ice-cold 0.9% saline solution. Any visible fat and connective tissue as well as the atria were removed, and the ventricles were frozen in liquid nitrogen and stored at −80 °C until further use. Hearts (*10*−*15*) were pooled for each SR preparation, powdered under liquid nitrogen, and homogenized in buffer A containing 20 mM Tris/maleate and 0.3 M sucrose (pH 7.0). The homogenate was centrifuged at 1000*g* for 15 min, and the pellet was rehomogenized in buffer A and spun at 1000*g* for 10 min. The obtained pellet was resuspended in buffer A, and an aliquot (pellet A) was stored at −80 °C. After an additional spin at 10000*g* for 20 min (pellet B), the supernatant was filtered through four layers of cheesecloth, and 1 M KCl was added to obtain a final concentration of 0.6 M KCl. After incubation at 4 °C for 15 min, the solution was centrifuged at 100000*g* for 1 h, and the supernatant was recentrifuged at 100000*g* for 1 h. The final pellet was resuspended in buffer A and stored at −80 °C (pellet C). Five SR preparations of phospholamban-deficient or wild-type hearts were obtained, using this method. The protein amount was determined by the Bio-Rad method, and the yield was 2.5−4.0 mg of enriched SR membranes/g of wet weight of myocardium. Pellets A, B, and C were processed in parallel to assess the enrichment of SR membranes, utilizing quantitative immunoblotting of SERCA2 and phospholamban (*5*). For the Coomassie Brilliant Blue staining (0.25%), the SR membrane preparations were subjected to 13% SDS−PAGE. The densitometric signal at ∼110 kDa was used to estimate the amount of SR Ca^{2+}-ATPase protein as compared to the total protein in the SR preparations. The presence of SERCA2 at ∼110 kDa was verified using immunoblotting, as previously described (*5*).

Sarcoplasmic Reticulum $^{45}Ca^{2+}$-Uptake. The sarcoplasmic reticulum-enriched preparations were diluted in buffer A to obtain a final concentration of 0.3 mg/mL. Ca^{2+} uptake rates were measured by the Millipore filtration technique, as previously described (*4*). The reaction mixture contained 40 mM imidazole /HCl (pH 7.0), 100 mM KCl, 5 mM $MgCl_2$, 5 mM NaN_3, 5 mM potassium oxalate, 0.5 mM EGTA, 1 μM ruthenium red, and various Ca^{2+} concentrations ranging between pCa 8.0 and 5.5. The SR membranes were incubated for 2 min at 37 °C in the reaction mixture, and Ca^{2+}-uptake was initiated by the addition of ATP (final concentration of 5 mM). The rates of Ca^{2+}-uptake were calculated by least-squares linear regression analysis of the 30-, 60-, and 90-s values of Ca^{2+}-uptake. The nonspecific uptake, obtained in the absence of ATP, was subtracted from the specific Ca^{2+} uptake at each time point. Furthermore, to examine whether any passive Ca^{2+} flux occurred across the SR vesicles during the Ca^{2+}-uptake assay, initial rates of Ca^{2+}-uptake were measured for 1 min at pCa 5.5 corresponding to V_{max} values, and two pCa (6.9 and 7.2) in the range where the decreased efficiency of the SR Ca^{2+} transport was observed (Figure 1). Initial uptake rates were inhibited by adding thapsigargin (100 nM) at 1 min after initiation of the reaction, and the SR Ca^{2+} load was subsequently assessed over 10 min. Upon inhibition of SERCA, the level of SR Ca^{2+} load remained constant up to 10 min in both wild-type and phospholamban-deficient hearts (Figure 1). Thus, there was no apparent passive Ca^{2+} flux from wild-type and phospholamban-deficient SR vesicles in the presence of oxalate.

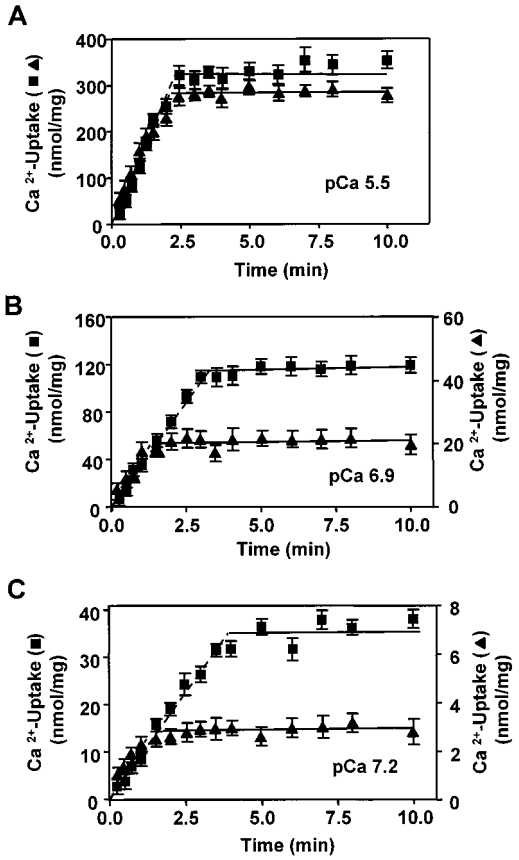

FIGURE 1: Ca^{2+}-uptake in phospholamban-deficient (■) and wild-type (▲) SR preparations at several pCa. The applied Ca^{2+} concentrations were chosen to obtain initial Ca^{2+}-uptake rates in the V_{max} range (pCa 5.5; panel A) and at pCa, where the decreased efficiency of the SR Ca^{2+}-ATPase was observed (pCa 6.9; panel B and pCa 7.2, panel C). Thapsigargin (100 nM) was added at 1 min after initiation of the reaction to inhibit the SR Ca^{2+}-ATPase. SR Ca^{2+} load was monitored over 10 min using the Millipore filtration method. Three SR preparations were used, and experiments were performed in duplicates. Values are means ± SEM.

Sarcoplasmic Reticulum Ca^{2+}-ATPase Activity. The initial rates of ATPase activity were determined by measuring the Ca^{2+}-dependent liberation of phosphate, using malachite green (*20*). The reaction conditions were identical to those utilized in the Ca^{2+} uptake assay. The SR membranes were incubated in the reaction mixture for 2 min at 37 °C, and ATPase activity measurements were initiated upon addition of ATP (5 mM final concentration). The ATP hydrolysis rates were determined by least-squares linear regression analysis of the 30-, 60-, and 90-s values of Ca^{2+}-ATPase activity.

In Vitro Phosphorylation of Cardiac Wild-Type Sarcoplasmic Reticulum Enriched Preparations. Phosphorylation of wild-type cardiac SR preparations was performed as previously described (*21*). Briefly, cAMP-dependent protein kinase (PKA) phosphorylation was carried out at 30 °C in 5 mL of reaction mixture containing 15 μg/mL protein, 50 mM K^+ phosphate buffer (pH 7.0), 10 mM $MgCl_2$, 5 mM NaF, 0.5 mM EGTA, 0.1 mM ATP, and 1000 units of PKA catalytic subunit (Sigma). The reaction was terminated after 2 min by adding 2 vol of ice-cold solution, containing 20 mM Tris/maleate (pH 7.0) and 0.1 M KCl. The phosphorylated SR membranes were centrifuged at 100000*g* for 30 min at 4 °C. The pellet was resuspended in Tris/maleate (pH 7.0), and an aliquot was evaluated for the recovered protein amount, using the Bio-Rad method, based on the method of Bradford (*22*). Control SR membranes were treated under identical conditions but in the absence of PKA catalytic subunit.

Thapsigargin-Sensitive Sarcoplasmic Reticulum Ca^{2+}-Uptake and Ca^{2+}-ATPase Activities. Sarcoplasmic reticulum-enriched membranes were incubated in the Ca^{2+}-uptake/ATPase reaction mixture containing thapsigargin, but not ATP, for 10 min at 37 °C. Subsequently, the reactions were initiated upon addition of ATP. The Ca^{2+}-uptake and Ca^{2+}-ATPase rates were obtained as described above. The thapsigargin-sensitive, SR-specific Ca^{2+}-uptake and Ca^{2+}-ATPase activity rates were calculated by subtracting the values obtained in the presence of thapsigargin from the corresponding rates of Ca^{2+}-uptake and Ca^{2+}-ATPase activities in the absence of thapsigargin.

MATERIALS AND METHODS

Protein kinase A catalytic subunit, malachite green oxalate, thapsigargin, and ruthenium red were obtained from Sigma-Aldrich, St. Louis, MO. All other chemicals were of the best analytical grade commercially available.

Statistical Analysis. Data are presented as means ± SEM. The number *n* indicates the number SR preparations unless otherwise stated. Statistical analysis was performed by student t-test for paired and unpaired observations. The nonlinear fit for the initial rates of Ca^{2+}-uptake and Ca^{2+}-ATPase activity was obtained using the Hill equation for a variable slope: $Y = V_{min} + (V_{max} - V_{min})/[1+10^{((\log[EC50]-\log[Ca])n)}]$ and the software program Prism Graphs Pad, version 3.0. Values of $p < 0.05$ were considered as statistically significant.

RESULTS

Sarcoplasmic reticulum-enriched microsomal preparations were isolated from wild-type and phospholamban-deficient hearts by differential centrifugation. The levels of SERCA2 were 10 ± 3% and 10 ± 3% of total protein in wild-type and phospholamban-deficient preparations, respectively, as revealed by Coomassie Brilliant Blue staining of SDS gels (Figure 2, panel A, inset). Furthermore, quantitative immunoblotting was used to determine the levels of SERCA2 and phospholamban in mouse microsomal preparations relative to cardiac homogenates. Enrichment of these proteins was 4.5-fold in the membrane preparations (pellet C) as compared to homogenates. The pellets (A and B), obtained during the isolation procedure, exhibited only minimal levels of SERCA2 or phospholamban (<10% of homogenate, data not shown). Thus, the relative ratio of phospholamban to SERCA2 in SR-enriched preparations remained similar to that in cardiac homogenates.

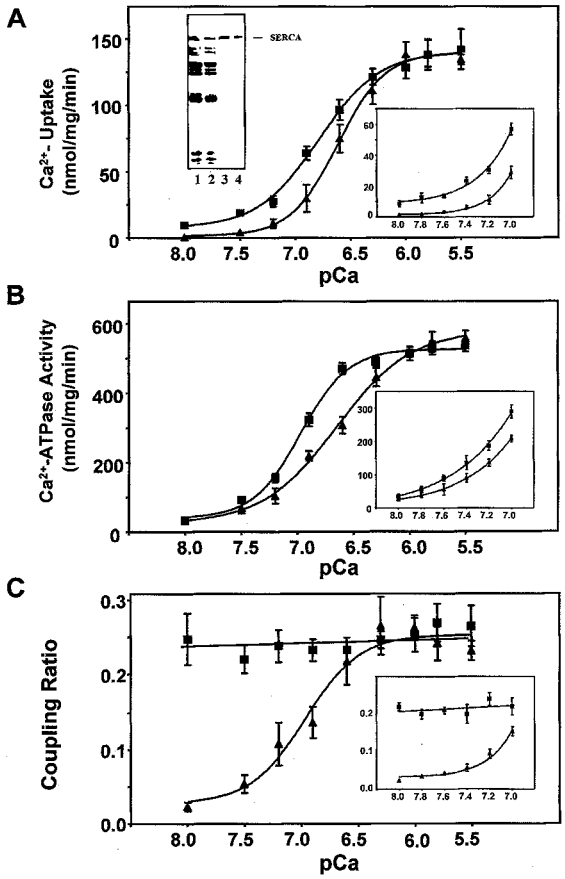

FIGURE 2: Initial rates of Ca^{2+}-uptake and Ca^{2+}-ATPase in phospholamban-deficient (■) and wild-type (▲) SR preparations. Five SR preparations, each consisting of 10−15 pooled mouse hearts from wild-type and phospholamban-deficient mice, were used to determine the initial rates of Ca^{2+}-uptake (A) and Ca^{2+}-ATPase (B) in duplicates or triplicates. The apparent coupling ratio (C) was calculated by dividing the rates of Ca^{2+} transported by the rates of ATP hydrolyzed at each pCa. The left inset in panel A shows Coomassie Brilliant Blue stained gels (lanes 1 and 2) and immunoblots (lanes 3 and 4) of wild-type SR preparations (50 μg for lanes 1 and 3, and 30 μg for lanes 2 and 4). The right insets in panels A−C represent Ca^{2+}-uptake rates, Ca^{2+}-ATPase activity, and coupling ratios at various low Ca^{2+} concentrations (pCa: 8.0−7.0; $n = 3$ preparations, performed in triplicates). Values are means ± SEM.

Wild-type and phospholamban-deficient SR were assayed for the initial rates of Ca^{2+}-uptake and Ca^{2+}-ATPase activity over a wide range of $[Ca^{2+}]$, similar to those present in the muscle cell during relaxation and contraction. Ruthenium red was included in the assays to inhibit the SR Ca^{2+}-release

Table 1: Calcium Concentration for Half-Maximal Response (EC_{50}) and Maximal Rates of Ca^{2+}-Uptake and Ca^{2+}-ATPase (V_{Max}) in Wild-Type and Phospholamban-Deficient SR Preparations[d]

	Ca^{2+}-ATPase activity		$^{45}Ca^{2+}$-uptake	
	EC_{50}	V_{max}	EC_{50}	V_{max}
WT	0.23 ± 0.04	578 ± 29	0.24 ± 0.04	140 ± 3
PLB-KO	0.11 ± 0.02[a]	538 ± 18	0.14 ± 0.03[a]	141 ± 3
WT (control)	0.20 ± 0.04	356 ± 14	0.22 ± 0.03	103 ± 2
WT + PKA	0.14 ± 0.03[b]	347 ± 11	0.14 ± 0.02[b]	102 ± 6
WT + Th	0.25 ± 0.04	178 ± 11	0.25 ± 0.02	134 ± 12
PLB-KO + Th	0.10 ± 0.04[c]	167 ± 13	0.14 ± 0.02[c]	137 ± 11

[a] $p < 0.05$ vs WT. [b] $p < 0.05$ vs WT (control). [c] $p < 0.05$ vs WT + Th. [d] Ca^{2+}-uptake and Ca^{2+}-ATPase activities were determined in wild-type (WT) and phospholamban-deficient (PLB-KO) SR preparations under identical conditions. Data are means ± SEM of 3−5 SR preparations each assayed in triplicates. PKA: catalytic subunit of protein kinase A; WT (control): control for PKA experiments; +Th: thapsigargin-sensitive Ca^{2+}-uptake and Ca^{2+}-ATPase activity; EC_{50} in μmol/L; V_{max} in nmol mg^{-1} min^{-1}.

channel (*23*). A dose−response curve of ruthenium red versus the initial rates of mouse cardiac SR Ca^{2+}-uptake at pCa 5.5 indicated that maximal inhibition occurred at 1 μM ruthenium red, and this dose was included in the reaction assays. The initial rates of both Ca^{2+}-uptake and Ca^{2+}-ATPase were significantly higher in phospholamban-deficient SR preparations at low [Ca^{2+}], resulting in an overall decrease in the apparent EC_{50} of the Ca^{2+}-uptake and Ca^{2+}-ATPase activities as compared to wild-type SR (Figure 2, panels A and B). However, the maximal rates of Ca^{2+}-uptake and Ca^{2+}-ATPase (V_{max}) were similar between the two groups (Table 1).

The apparent coupling ratio was then calculated by dividing the Ca^{2+} transport rates by the ATP hydrolysis rates at each pCa. We observed a sigmoidal relationship, with low values at low [Ca^{2+}] and higher values at high [Ca^{2+}] for wild-type cardiac SR (Figure 2, panel C). However, in phospholamban-deficient SR, the apparent coupling ratio was constant, and it exhibited values similar to those obtained at high [Ca^{2+}] in wild-type SR (Figure 2, panel C). To further confirm the observed differences in the coupling ratio between wild-type and phospholamban-deficient SR at low [Ca^{2+}] the initial rates of Ca^{2+}-uptake and Ca^{2+}-ATPase were assessed at several pCa values between 8.0 and 7.0 (Figure 2, panels A and B, insets). The apparent coupling ratio appeared to increase with increasing [Ca^{2+}] in wild-type, while it remained constant and Ca^{2+}-independent in phospholamban-deficient SR preparations at all Ca^{2+} concentrations tested (Figure 2, panel C, inset). These findings indicate that phospholamban regulates the apparent coupling ratio of Ca^{2+} transported per ATP hydrolyzed.

To obtain further evidence on the functional role of phospholamban, SR membrane preparations from wild-type mouse hearts were phosphorylated by the catalytic subunit of protein kinase A (PKA). Control membranes were treated in parallel but in the absence of PKA. Phosphorylation of phospholamban resulted in significant increases in the initial rates of Ca^{2+}-uptake and Ca^{2+}-ATPase at low pCa (Figure 3, panels A and B), which was associated with a decrease in their EC_{50} values for Ca^{2+}, as compared to nonphosphorylated SR (Figure 3 and Table 1). There was no effect of phosphorylation on the V_{max} of Ca^{2+}-uptake and Ca^{2+}-ATPase activities. However, both of these values were 35% lower than those observed in untreated wild-type SR (Figure 2, panels A and B). These lower activities appeared to be due to the preincubation conditions, since the rates were similar between phosphorylated and nonphosphorylated SR. Calculations of the apparent coupling ratio from these data indicated a Ca^{2+}-dependent relationship in wild-type SR, similar to Figure 2, panel C. However, upon phosphorylation of phospholamban, the coupling ratio exhibited a constant, Ca^{2+}-independent pattern, similar to the one observed at high [Ca^{2+}] in wild-type SR preparations (Figure 3, panel C). Thus, phosphorylation of phospholamban had similar effects as ablation of this protein on the apparent coupling ratio of the SR Ca^{2+} transport system.

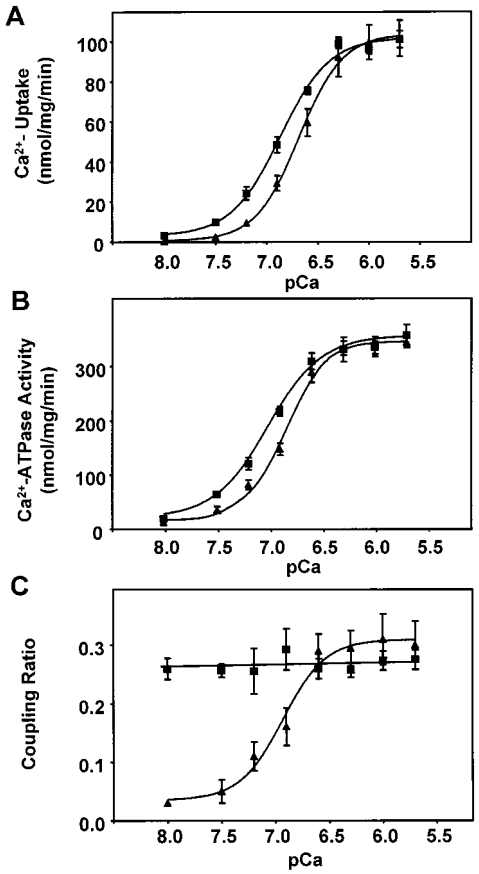

FIGURE 3: Effect of protein kinase A on wild-type SR. Wild-type SR preparations (▲) were phosphorylated by the catalytic subunit of PKA (■), and the initial rates of Ca^{2+}-uptake (A) and Ca^{2+}-ATPase (B) were assessed over a wide range of pCa. The apparent coupling ratio (C) was calculated by dividing the Ca^{2+}-uptake rates by the corresponding Ca^{2+}-ATPase rates at each pCa. Values represent the mean ± SEM of three SR preparations, assayed in triplicates.

Since microsomal preparations have been reported to contain Ca^{2+}-dependent ATPases, other than the SR-associated enzyme (*24*), we used thapsigargin (*25*) to differentiate between these activities. Maximal inhibition of oxalate-supported Ca^{2+}-uptake rates occurred at 100 nM thapsigargin, consistent with previous observations (*25*). Thus, Ca^{2+}-uptake and Ca^{2+}-ATPase activities were assayed, in the presence of 100 nM thapsigargin, especially since higher concentrations (≥ 1 μM) have been reported to affect the composition and leakage of SR vesicles (*26*). The SR Ca^{2+}-uptake rates were completely inhibited, while total Ca^{2+}-ATPase activity

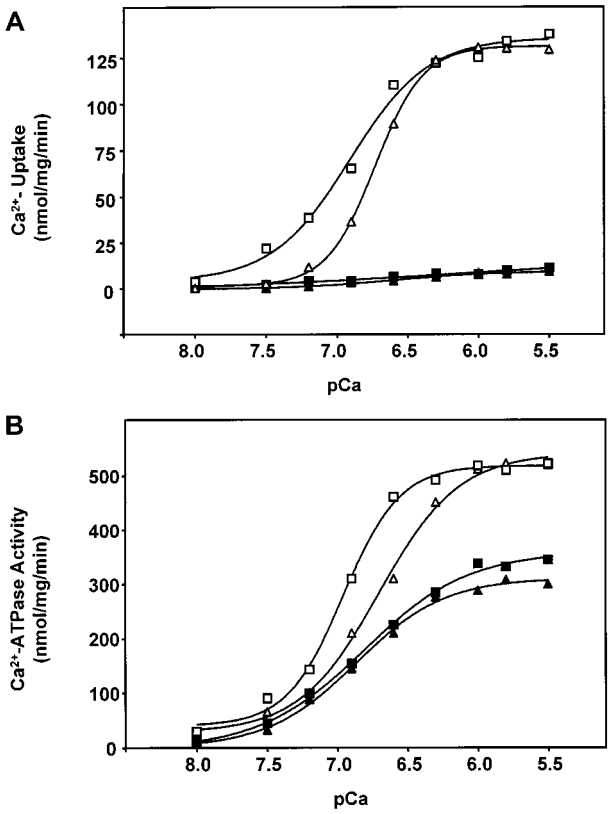

FIGURE 4: Representative experiment on the effect of thapsigargin (100 nM) on the initial rates of Ca^{2+}-uptake and Ca^{2+}-ATPase activity in phospholamban-deficient and wild-type SR preparations. Phospholamban-deficient (□, ■) and wild-type (△, ▲) SR-enriched preparations were assayed for the initial rates of Ca^{2+}-uptake and Ca^{2+}-ATPase activity in the absence (open symbols) or presence (closed symbols) of thapsigargin over a wide range of Ca^{2+} concentrations. Values represent the mean of triplicate assays.

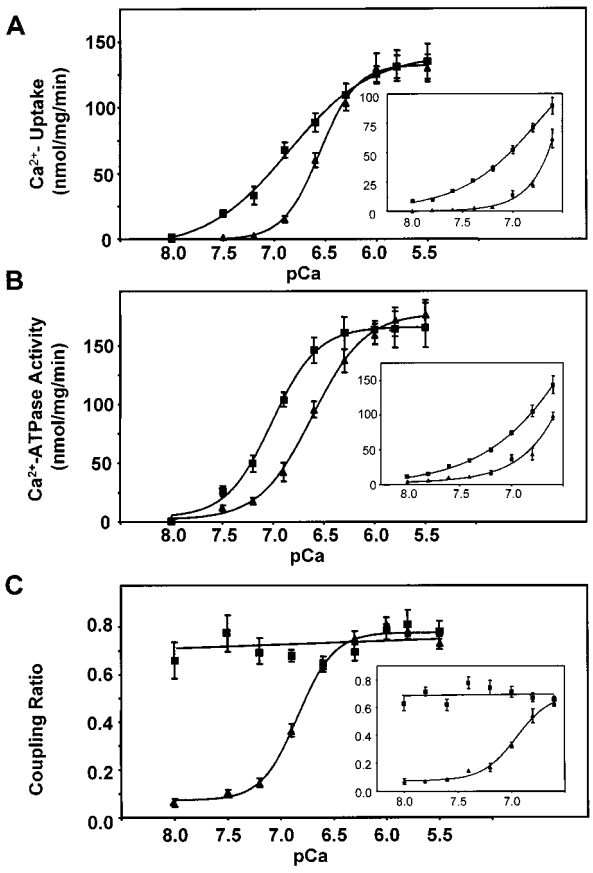

FIGURE 5: Thapsigargin-sensitive Ca^{2+}-uptake and Ca^{2+}-ATPase activities in phospholamban-deficient (■) and wild-type SR preparations (▲). Five SR preparations (10−15 pooled mouse hearts/preparation) were used, and Ca^{2+} -uptake (A) or Ca^{2+}-ATPase (B) assays were performed in triplicate. The apparent coupling ratio (C) was calculated by dividing the rates of Ca^{2+} transported by the rates of ATP hydrolyzed at each pCa. The insets represent Ca^{2+}-uptake rates, Ca^{2+}-ATPase activity, and coupling ratios at various low Ca^{2+} concentrations (pCa: 8.0−6.6). Values are means ± SEM.

was reduced by 35% in the presence of 100 nM thapsigargin in both wild-type and phospholamban-deficient preparations (Figure 4). To obtain the SR-dependent Ca^{2+}-uptake and Ca^{2+}-ATPase activities, the thapsigargin-sensitive Ca^{2+}-uptake and Ca^{2+}-ATPase activity rates were then subtracted from the respective rates obtained in the absence of thapsigargin (Figure 5). The maximal velocities (V_{max}) of SR Ca^{2+}-uptake and Ca^{2+}-ATPase were similar between wild-type and phospholamban-deficient SR preparations (Figure 5, panels A and B). Furthermore, the V_{max} values of Ca^{2+}-uptake were similar to those obtained in the absence of thapsigargin, while the V_{max} of SR Ca^{2+}-ATPase was 3.1-fold lower in both wild-type and phospholamban-deficient SR (Table 1). When the apparent coupling ratio of Ca^{2+} transported per ATP hydrolyzed was calculated, a Ca^{2+}-dependent pattern was obtained for wild-type SR with a maximal value of 0.82 at high [Ca^{2+}]. However, in phospholamban-deficient SR, the value of 0.82 was observed at all [Ca^{2+}] (Figure 5, panel C). To verify the differences in the apparent coupling ratios between wild-type and phospholamban-deficient SR, an additional series of experiments with more points at pCa 8.0 to 6.6 was conducted (Figure 5, panels A and B, insets). The apparent coupling ratio increased with increasing [Ca^{2+}] in wild-type SR, but it remained constant in phospholamban-deficient SR (Figure 5, panel C, inset). A similar constant coupling ratio would be expected upon phosphorylation of phospholamban in wild-type SR (see above).

DISCUSSION

The present study suggests that phospholamban may regulate the apparent efficiency of the SR Ca^{2+} transport system, especially at low or diastolic [Ca^{2+}]. The generation of a phospholamban-deficient mouse model coupled with biochemical studies on SR Ca^{2+} transport and Ca^{2+}-ATPase activities, allowed us to identify this regulatory function of phospholamban in cardiac SR. In this study, SR-enriched membrane preparations were used, and cAMP-dependent phosphorylation or ablation of phospholamban was associated with decreases in the apparent EC_{50} for Ca^{2+} of Ca^{2+}-uptake, similar to previous observations, using mouse cardiac homogenates (*4*). This effect of phospholamban was also consistent with reports in other species, such as dog (*27*), rabbit (*28*), and rat (*29*). Furthermore, phospholamban phosphorylation or ablation resulted in a decrease in the EC_{50} for Ca^{2+} of the murine SR Ca^{2+}-ATPase. The decreases in the EC_{50} values of SR Ca^{2+}-uptake and Ca^{2+}-ATPase were similar (Table 1), while there were no alterations on the V_{max} of these activities. To obtain an apparent coupling ratio for the SR Ca^{2+}-transport system, we divided the initial rates of Ca^{2+}-uptake by those of Ca^{2+}-ATPase, since these activities were assayed under identical conditions. We observed that the ratio of Ca^{2+} transported per ATP hydrolyzed was [Ca^{2+}]-

dependent in wild-type SR, but phosphorylation or ablation of phospholamban resulted in a [Ca^{2+}]-independent ratio. Furthermore, the highest value of the coupling ratio in wild-type SR was obtained at high [Ca^{2+}] or upon maximal activation of the Ca^{2+}-transport system. This coupling ratio value was similar to that obtained upon removal of the phospholamban inhibitory effects, elicited by phosphorylation or ablation of the protein. Thus, phospholamban appears to regulate the efficiency of the SR Ca^{2+}-transport system at low [Ca^{2+}].

Diminished coupling efficiency was also previously observed in the presence of furylacryloyl phosphate (*30*), acidic conditions (*31*), high alkaline EGTA (*32*), and upon tryptic digestion (*33*), changing the aminophospholipid composition of the SR (*34*) or inactivating the SR Ca^{2+}-ATPase, which may result in Ca^{2+}-permeable channel formation (*35*). However, none of these conditions were present in our assay system, and the maximal activity and uptake rates were similar in wild-type and phospholamban-deficient SR preparations. Furthermore, no passive Ca^{2+} flux was observed in the SR preparations after complete inhibition of the SR Ca^{2+}-ATPase by thapsigargin. The use of thapsigargin to assess the SR-specific Ca^{2+}-ATPase activity in the mouse microsomal preparations revealed an apparent coupling ratio of 0.82 for Ca^{2+} transported per ATP hydrolyzed at high [Ca^{2+}]. This value is among the highest coupling ratios, previously reported, which varied between 0.08 and 0.88 for SR-enriched preparations (*11*, *36*−*39*). However, higher values (0.5−2.0) have been obtained in reconstitution experiments of SERCA2 and phospholamban or expression systems of these two proteins (*40*−*42*). It is interesting to note that upon examination of published reports, a similar pattern of alterations in the apparent coupling ratio of Ca^{2+} transported per ATP utilized was also obtained in two other studies (*39*, *40*). In canine cardiac SR preparations, a change in the coupling ratio from 0.06 at pCa 7.8 to 0.63 at pCa 6.7 was observed (*39*), and it was suggested that this may be due to the presence of oxalate, which would not sufficiently precipitate calcium at low pCa. However, in our study, both SR preparations were treated under identical conditions, and the differences in coupling ratio were obtained even when the initial rates of Ca^{2+}-uptake were similar between wild-type and phospholamban-deficient SR.

Three independent lines of evidence indicate that the observed reduction in the apparent coupling ratio cannot be attributed to systematic errors, which may be due to the relatively low Ca^{2+}-uptake and Ca^{2+}-ATPase rates obtained at low [Ca^{2+}] (below 320 nM). First, any such error should occur in all cases, but coupling ratio changes were obtained only in dephosphorylated wild-type SR and not in either phospholamban-deficient or phosphorylated wild-type SR (Figures 2, 4, and 5). Second, an additional series of experiments with more points at pCa 8 to 6.6 showed consistent results (Figures 2 and 5 insets). Third, the coupling ratio is reduced by 50% at pCa 6.9, where levels of SR Ca^{2+}-ATPase and Ca^{2+}-uptake rates are well above the detection thresholds of the assay (25 and 13% of V_{max}, respectively). Thus, a reduced coupling ratio at low [Ca^{2+}] seems to be a genuine property of the SR Ca^{2+}-ATPase associated with dephosphorylated phospholamban. The mechanism by which phospholamban mediates its regulatory effects on the SR Ca^{2+}-ATPase may involve a direct physical interaction

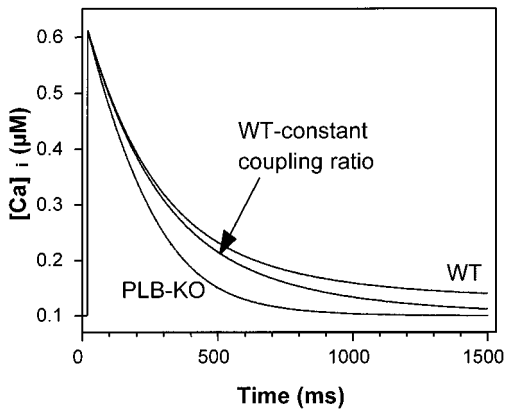

FIGURE 6: Simulated single-cell Ca^{2+} transients in phospholamban-deficient and wild-type cardiac myocytes. These curves are based on quantitative analysis and equations for intact cell Ca^{2+} dynamics in voltage-clamped ventricular myocytes, as developed by Shannon et al. (*48*). Total cytosolic Ca^{2+} was driven by the SR Ca^{2+} release, and free $[Ca]_i$ was obtained by numerical integration, which included Ca^{2+} buffering (*51*) and Ca^{2+} transport by the SR. Cytosolic and SR Ca^{2+} buffering, SR Ca^{2+} release (83 μmol/L cytosol), and V_{max} for the SR Ca^{2+}-ATPase [178 μmol (L cytosol)$^{-1}$ s^{-1}] were assumed to be the same in all three cases. The phospholamban-deficient (PLB-KO) curve used $EC_{50} = 98$ nM and $n_H = 2.014$, which produced a $t_{1/2}$ of 150 ms, similar to previous observations (*52*). The lower wild-type (WT) curve used $EC_{50} = 245$ nM, $n_H = 1.797$, as derived from Figure 5, panel B. The top wild-type curve used the same EC_{50} and n_H, but the forward transport rate was multiplied by the measured coupling ratio in Figure 5, panel C, which was normalized to a maximum value of 1 (i.e., $0.9043/\{1 + (145/[Ca]_i)^{2.55}\} + 0.0957$). The simulation indicates that uncoupling of the SR Ca^{2+} transport significantly prolongs relaxation.

between the two proteins (*17*, *43*), electrostatic modification of the SR membrane potential (*44*), or alterations in lipid chain motion (*45*) resulting in modulation of the membrane fluidity. Alternatively, phospholamban may mediate the apparent Ca^{2+} leak itself, through formation of ion pores by its pentameric structure (*18*, *19*). However, studies in reconstituted systems of the SR Ca^{2+}-ATPase with phospholamban did not detect any significant Ca^{2+} leakage promoted in the presence of phospholamban (*46*). Consistent with these findings, phospholamban-deficient and wild-type SR preparations exhibited no passive flux in the presence of oxalate. Alternatively, phospholamban may regulate the "backflux" of Ca^{2+} through the Ca^{2+} pump, which may operate in a reverse mode, as recently suggested (*47*, *48*).

An important question is whether the observed alterations in the SR Ca^{2+} transport efficiency would have an impact on intracellular Ca^{2+}-handling in vivo. To address this, single-cell Ca^{2+} transients [including Ca^{2+} current, reversible SR Ca^{2+} pump, SR Ca^{2+} leak and cytosolic as well as intra-SR Ca^{2+} buffering (*48*)] were simulated (Figure 6). The reduced SR Ca^{2+}-ATPase affinity for Ca^{2+} and coupling ratio in the presence of phospholamban appear to contribute additively to slowing cellular $[Ca]_i$ decline. The reduced coupling especially prolongs the late phase of $[Ca]_i$ decline and relaxation, which may extend myofilament interaction (and ATP consumption) and alter other Ca^{2+}-dependent processes (e.g., Ca^{2+} current, SR Ca^{2+} release channels and Na^+/Ca^{2+} exchange). The amount of ATP required to transport the same number of Ca^{2+} ions is also increased, raising the overall energy cost of Ca^{2+} cycling. Finally, the lower energetic efficiency of the SR Ca^{2+} pump at diastolic

[Ca^{2+}] in the presence of phospholamban could reduce the maximal free [Ca^{2+}] gradient that the pump can establish, which would limit total SR Ca^{2+} load and the fraction of SR Ca^{2+} released during a twitch (*48*−*50*). Thus, the ability of dephosphorylated phospholamban to reduce SR Ca^{2+} pump coupling may have far-reaching physiological implications.

In summary, our findings suggest that dephosphorylated phospholamban reduces the affinity of the SR Ca^{2+}-ATPase as well as the apparent efficiency of the Ca^{2+}-transport system in cardiac SR. The reduced coupling ratio at low [Ca^{2+}] would prolong especially the late phase of $[Ca]_i$ decline, which might result in elevated diastolic $[Ca]_i$, upon repeated Ca^{2+} transients, leading to increased cardiac diastolic tension and consequent energy consumption. Thus, phosphorylation of phospholamban resulting in enhancement of the apparent SR Ca^{2+} transport coupling ratio may provide an additional mechanism to prevent increases in heart rate-dependent diastolic tension during β-adrenergic stimulation.

REFERENCES

1. Kadambi, V. J., and Kranias, E. G. (1997) *Biochem. Biophys. Res. Commun. 239*, 1−5.
2. Simmerman, H. K., and Jones, L. R. (1998) *Physiol. Rev. 78*, 921−47.
3. Koss, K. L., and Kranias, E. G. (1996) *Circ. Res. 79*, 1059−63.
4. Luo, W., Grupp, I. L., Harrer, J., Ponniah, S., Grupp, G., Duffy, J. J., Doetschman, T., and Kranias, E. G. (1994) *Circ. Res. 75*, 401−9.
5. Chu, G., Luo, W., Slack, J. P., Tilgmann, C., Sweet, W. E., Spindler, M., Saupe, K. W., Boivin, G. P., Moravec, C. S., Matlib, M. A., Grupp, I. L., Ingwall, J. S., and Kranias, E. G. (1996) *Circ. Res. 79*, 1064−76.
6. Desai, K. H., Schauble, E., Luo, W., Kranias, E., and Bernstein, D. (1999) *Am. J. Physiol. 276*, H1172−7.
7. Dash, R., Slack, J. P., Grupp, I. L., Holder, D., Tilgmann, C., Tamura, T., Johnson, R., Gerdes, A. M., and Kranias, E. G. (1999) *Circulation 100*, 622 (abstract).
8. Hicks, M. J., Shigekawa, M., and Katz, A. M. (1979) *Circ. Res. 44*, 384−91.
9. MacLennan, D. H., Rice, W. J., and Green, N. M. (1997) *J. Biol. Chem. 272*, 28815−8.
10. Lindemann, J. P., Jones, L. R., Hathaway, D. R., Henry, B. G., and Watanabe, A. M. (1983) *J. Biol. Chem. 258*, 464−71.
11. Kranias, E. G., Garvey, J. L., Srivastava, R. D., and Solaro, R. J. (1985) *Biochem. J. 226*, 113−21.
12. Cantilina, T., Sagara, Y., Inesi, G., and Jones, L. R. (1993) *J. Biol. Chem. 268*, 17018−25.
13. Voss, J., Jones, L. R., and Thomas, D. D. (1994) *Biophys. J. 67*, 190−6.
14. Toyofuku, T., Kurzydlowski, K., Tada, M., and MacLennan, D. H. (1994) *J. Biol. Chem. 269*, 3088−94.
15. Sasaki, T., Inui, M., Kimura, Y., Kuzuya, T., and Tada, M. (1992) *J. Biol. Chem. 267*, 1674−9.
16. Simmerman, H. K., Kobayashi, Y. M., Autry, J. M., and Jones, L. R. (1996) *J. Biol. Chem. 271*, 5941−6.
17. Kimura, Y., Kurzydlowski, K., Tada, M., and MacLennan, D. H. (1997) *J. Biol. Chem. 272*, 15061−4.
18. Kovacs, R. J., Nelson, M. T., Simmerman, H. K., and Jones, L. R. (1988) *J. Biol. Chem. 263*, 18364−8.
19. Arkin, I. T., Adams, P. D., MacKenzie, K. R., Lemmon, M. A., Brunger, A. T., and Engelman, D. M. (1994) *EMBO J. 13*, 4757−64.
20. Van Veldhoven, P. P., and Mannaerts, G. P. (1987) *Anal. Biochem. 161*, 45−8.
21. Luo, W., Chu, G., Sato, Y., Zhou, Z., Kadambi, V. J., and Kranias, E. G. (1998) *J. Biol. Chem. 273*, 4734−9.
22. Bradford, M. M. (1976) *Anal. Biochem. 72*, 248−54.
23. Fleischer, S., and Inui, M. (1988) *Prog. Clin. Biol. Res. 273*, 435−50.
24. Inesi, G. (1985) *Annu. Rev. Physiol. 47*, 573−601.
25. Inesi, G., and Sagara, Y. (1992) *Arch. Biochem. Biophys. 298*, 313−7.
26. Tao, J., and Haynes, D. H. (1992) *J. Biol. Chem. 267*, 24972−82.
27. Lu, Y. Z., Xu, Z. C., and Kirchberger, M. A. (1993) *Biochemistry 32*, 3105−11.
28. Xu, A., and Narayanan, N. (1999) *Biochem. Biophys. Res. Commun. 258*, 66−72.
29. Chiesi, M., and Schwaller, R. (1994) *Biochem. Biophys. Res. Commun. 202*, 1668−73.
30. Inesi, G., Kurzmack, M., Nakamoto, R., de Meis, L., and Bernhard, S. A. (1980) *J. Biol. Chem. 255*, 6040−3.
31. Berman, M. C., McIntosh, D. B., and Kench, J. E. (1977) *J. Biol. Chem. 252*, 994−1001.
32. Duggan, P. F., and Martonosi, A. (1970) *J. Gen. Physiol. 56*, 147−67.
33. Stewart, P. S., and MacLennan, D. H. (1974) *J. Biol. Chem. 249*, 985−93.
34. Hidalgo, C., Petrucci, D. A., and Vergara, C. (1982) *J. Biol. Chem. 257*, 208−16.
35. Jilka, R. L., Martonosi, A. N., and Tillack, T. W. (1975) *J. Biol. Chem. 250*, 7511−24.
36. Kirchberger, M. A., and Antonetz, T. (1982) *J. Biol. Chem. 257*, 5685−91.
37. Ganguly, P. K., Pierce, G. N., Dhalla, K. S., and Dhalla, N. S. (1983) *Am J Physiol 244*, E528−35.
38. Xu, Z. C., and Kirchberger, M. A. (1989) *J. Biol. Chem. 264*, 16644−51.
39. Briggs, F. N., Lee, K. F., Wechsler, A. W., and Jones, L. R. (1992) *J. Biol. Chem. 267*, 26056−61.
40. Reddy, L. G., Jones, L. R., Cala, S. E., O'Brian, J. J., Tatulian, S. A., and Stokes, D. L. (1995) *J. Biol. Chem. 270*, 9390−7.
41. Kimura, Y., Kurzydlowski, K., Tada, M., and MacLennan, D. H. (1996) *J. Biol. Chem. 271*, 21726−31.
42. Mayer, E. J., McKenna, E., Garsky, V. M., Burke, C. J., Mach, H., Middaugh, C. R., Sardana, M., Smith, J. S., and Johnson, R. G., Jr. (1996) *J. Biol. Chem. 271*, 1669−77.
43. Autry, J. M., and Jones, L. R. (1997) *J. Biol. Chem. 272*, 15872−80.
44. Chiesi, M., and Schwaller, R. (1989) *FEBS Lett. 244*, 241−4.
45. Cornea, R. L., Jones, L. R., Autry, J. M., and Thomas, D. D. (1997) *Biochemistry 36*, 2960−7.
46. Stokes, D. L. (1997) *Curr. Opin. Struct. Biol. 7*, 550−6.
47. Feher, J. J., and Briggs, F. N. (1984) *Biophys. J. 45*, 1135−44.
48. Shannon, T. R., Ginsburg, K. S., and Bers, D. M. (2000) *Biophys. J. 78*, 322−33.
49. Santana, L. F., Kranias, E. G., and Lederer, W. J. (1997) *J. Physiol. (Lond) 503*, 21−9.
50. Shannon, T. R., Ginsburg, K. S., and Bers, D. M. (2000) *Biophys. J. 78*, 334−43.
51. Hove-Madsen, L., and Bers, D. M. (1993) *Am. J. Physiol. 264*, C677−86.
52. Li, L., Chu, G., Kranias, E. G., and Bers, D. M. (1998) *Am. J. Physiol. 274*, H1335−47.

BI001049K